

# Optical Sensors Based on Active Microcavities

Jun Yang and L. Jay Guo, *Member, IEEE*

**Abstract**—We propose an active optical sensor based on a microcavity with gain. Greatly improved sensitivity can be achieved in active microcavities as compared with passive high- $Q$  microcavities. We show that an active sensor using a gain-doped microsphere can provide  $10^4$ -fold narrower resonance linewidth than does a passive microcavity in the transmission spectrum. Such highly sensitive microcavity optical sensors can be used to detect low concentrations of chemicals or biomolecules in their surroundings. Our analysis shows that this type of compact active microcavity is sensitive to an effective refractive index change of the order of  $10^{-9}$ .

**Index Terms**—Active sensor, biosensor, microcavity, microdisk, microring, microsphere, whispering-gallery mode (WGM).

## I. INTRODUCTION

**M**INIATURE optical sensors for detecting biochemical analytes in gas or aqueous solution are undergoing fast development. Optical waveguide sensors using evanescent waves to interrogate the presence of analytes on a waveguide surface or in the surrounding environment typically rely on the detection of effective refractive index change. These sensors are attractive due to their robustness, compatibility with microfluidic handling, and their ability to provide high specificity using surface chemical modifications. But in order to detect very low concentrations or minute amounts of analytes, long waveguides are typically required in order to accumulate significant phase shift. This would also require a large amount of sample, which may not be readily obtainable in certain applications. On the other hand, sensors based on optical microcavities offer a unique advantage by reducing the size of the device by orders of magnitude, thereby significantly reducing the amount of sample needed for the detection. The resonance effect also provides an effective long interaction length for the sensor to achieve sufficient sensitivity. High quality-factor microcavities such as microspheres [1], [2], microdisks [3] using whispering-gallery mode (WGM) resonances, and microrings [4] with guided circulating modes have already been proposed and demonstrated for biosensor applications. The WGMs evanescent wave, established through total internal reflection, is affected by the change of the surrounding environment that results in the change of the effective refractive index of the WGM modes. To convert the resultant phase change of the WGM modes, one can use a tapered fiber to couple with the microsphere [Fig. 1(a)] and detect the resonance shift or the intensity change at fixed wavelength

Manuscript received March 20, 2005; revised September 30, 2005. This work was supported in part by the National Institute of Health, in part by the University of Michigan's Technology Transfer Office, and in part by the MUCI challenge fund.

The authors are with the Department of Electrical Engineering and Computer Science, University of Michigan, Ann Arbor, MI 48109 USA (e-mail: guo@eecs.umich.edu).

Digital Object Identifier 10.1109/JSTQE.2005.862953

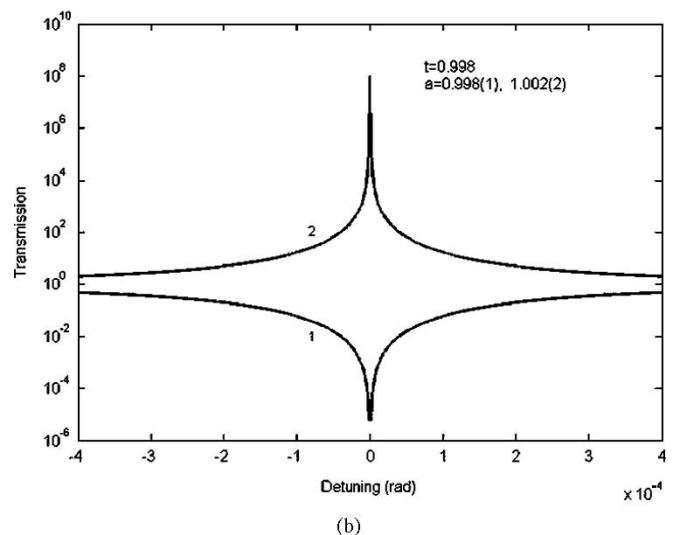
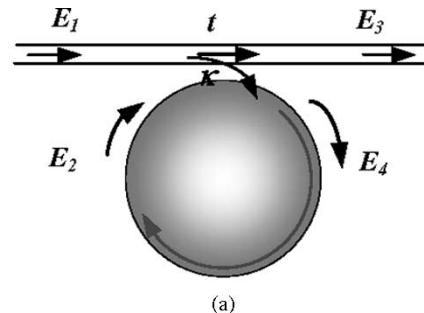


Fig. 1. (a) Schematic of a microsphere or microring resonator. (b) Transmission spectrum of the microcavity (curve 1,  $\alpha = t < 1$  corresponding to microcavity with loss at critical coupling; curve 2,  $\alpha t = 1$  for microcavity with gain at the lasing threshold).

from the transmission spectrum measured at the output end of the fiber.

The resonances of WGM modes for a microsphere coupled with a tapered fiber (or equivalently, a microdisk/microring coupled with an integrated optical waveguide) can be analyzed in terms of transmission through the coupled system, which is given by [5]

$$T = \left| \frac{E_3}{E_1} \right|^2 = \frac{\alpha^2 + t^2 - 2\alpha t \cos \phi}{1 + \alpha^2 t^2 - 2\alpha t \cos \phi} \quad (1)$$

where  $\phi = n_e \omega L / c$ ,  $\alpha$  = single-pass field attenuation factor,  $t$  = transmission coefficient,  $\omega$  = frequency,  $n_e$  = effective refractive index, and  $L$  = microcavity perimeter. The transmission spectrums are shown in Fig. 1(b) for microcavities with loss and gain, respectively.

From (1), we can obtain the bandwidth of the transmission resonances

$$\Delta\omega = \frac{2c}{\pi n_e R} \frac{1 - \alpha t}{\sqrt{\alpha t}} \approx \frac{c}{\pi n_e R} (\gamma^2 + \kappa^2) \quad (2)$$

and the quality factor

$$Q = \frac{\omega}{\Delta\omega} = \frac{\pi^2 n_e R}{\lambda} \frac{\sqrt{\alpha t}}{1 - \alpha t} \approx \left( \frac{1}{Q_{\text{ex}}} + \frac{1}{Q_{\text{in}}} \right)^{-1}. \quad (3)$$

Here,  $Q_{\text{ex}} = \pi l / \kappa^2 =$  external loss limited quality factor and  $Q_{\text{in}} = \pi l / \gamma^2 =$  intrinsic loss limited  $Q$  [6];  $\gamma^2 = 1 - \alpha^2 =$  single-pass loss coefficient,  $\kappa^2 = 1 - t^2 =$  coupling coefficient,  $l =$  mode number, and  $R =$  radius of microcavity. In (2) and (3), the approximation  $\gamma^2, \kappa^2 \ll 1$  is used, which is generally valid for low loss and high- $Q$  microcavities.

Passive cavities always have propagation losses [i.e.,  $\alpha < 1$  and curve 1 in Fig. 1(b)], which limits the attainable  $Q$ -factor and the achievable sensitivity in sensor applications. Special techniques can be used to reduce losses as demonstrated in [7], leading to improved  $Q$  of up to  $10^8$ . On the other hand, we notice from Fig. 1(b) that if the cavity has gain, a much narrower resonance line width can be achieved [curve 2 in Fig. 1(b)], resulting in a  $\omega / \Delta\omega$  much higher than that in the passive cavity case. This is the basis of an active sensor, where greatly improved sensitivity can be achieved by imparting gain to the resonator to achieve a higher active  $Q$ . A similar idea has been used previously in a grating distributed Bragg reflector (DBR) laser [8]. However, a microcavity with WGMs can provide higher  $Q$  than DBR cavities do. Also, compared with a DBR laser sensor, active WGM microcavities do not require an additional element to produce the evanescent field, which makes the system much simpler to implement. In addition, a more compact sensor can be fabricated by using integrated microdisk or microring cavities.

This paper is devoted to the design and calculation of active sensors based on polymer microspheres that are coupled with tapered cylindrical waveguides. We will show that active sensors can achieve much narrower linewidth at the lasing condition, and therefore can provide a much higher active  $Q$  factor. We will also discuss how to optimally choose some of the critical parameters in order to achieve suitable  $Q$ 's and a maximum coupling between the polymer microsphere and the tapered waveguide.

## II. PRINCIPLE OF ACTIVE MICROCAVITY SENSORS

In this section, we analyze an active sensor based on a dye-doped polymer microsphere coupled with a tapered cylindrical polymer waveguide. We assume the polymer to be polystyrene without losing generality. First, we will evaluate the lasing threshold and the linewidth to show that a  $10^4$ -fold narrower linewidth can be achieved in active microcavities as compared to passive ones. Second, we will derive a relationship between the spectrum line shift and the environment's index change by using perturbation approximation and mode volume evaluation. By so doing, we can obtain the minimum index change that can be detected by such a sensor system. Note that the device proposed here is intended for low level detection, such as to detect ultralow concentrations of analytes in a solution. In such

cases, the low densities of analyte molecules will only present a small perturbation to the WDM modes, and the influence of the substance to the dielectric function of the microsphere can be neglected. Therefore, we only consider its effect on the effective index of the WDM modes.

Unless otherwise noted, the following parameters are used in the calculations: 1) the refractive index of polystyrene material is assumed to be  $n_s = 1.59$  at wavelengths of 530 nm and 580 nm; 2) the environment surrounding the microsphere is assumed to be water with refractive index  $n_0 = 1.33$ ; and 3) the gain medium is Rhodamine-6G with the following typical parameters: pump wavelength  $\lambda_p = 530$  nm, lasing wavelength  $\lambda_l = 580$  nm, excited state life time  $\tau = 3.7 \times 10^{-9}$  s and stimulated emission cross section  $\sigma_e = 1.2 \times 10^{-16}$  cm<sup>2</sup> [9]. In the device operation, both the pump light and signal light will be introduced from the same input port of the optical fiber. The resonance spectrum of the signal light will be measured from the output port of the fiber. The output due to pump light will not interfere with the measurement because it is at a very different frequency.

### A. Lasing Threshold and Linewidth

Note that an active sensor on resonance is essentially a laser system with the sensing application taking advantage of the environmental sensitivity of this system. A glass microsphere laser using Er-doped gain media and coupled with tapered optical fiber has been successfully demonstrated [10]. The analysis of laser threshold behavior can be found in classical textbooks [11]. The population inversion density at the threshold is

$$\Delta N_{\text{th}} = \frac{\ln(G_{\text{th}})}{\sigma_e \cdot 2\pi R} \quad (4)$$

where the threshold gain  $G_{\text{th}} = 1/L_{\text{loss}}$ ,  $L_{\text{loss}}$  is the total cavity loss per round trip, and  $\sigma_e$  is the stimulated emission cross section. The threshold pumping power is

$$P_{\text{th}} = \frac{\Delta N_{\text{th}} V h c}{\chi \tau \lambda_p} \quad (5)$$

where  $\chi$  is the pumping efficiency and  $V$  the pumping mode volume. For our case, we take 50% pumping efficiency ( $\chi = 0.5$ ) and  $V \approx (3\lambda_p)^2 \cdot 2\pi R$  [12]. Thus, we have

$$P_{\text{th}} = \frac{18 \ln(1/L_{\text{loss}}) h c \lambda_p}{\sigma_e \tau}. \quad (6)$$

With these results, we can further obtain the lasing linewidth. The linewidth is calculated according to the Schawlow-Townes formula for a laser oscillator [11]

$$\Delta\omega_{\text{osc}} = \frac{N_{2\text{th}}}{\Delta N_{\text{th}}} \frac{2\pi \hbar \omega_0}{P_{\text{osc}}} (\Delta\omega_c)^2. \quad (7)$$

Here, the spectrum linewidth of the passive cavity resonance is  $\Delta\omega_c = \omega_0 / Q$ , and we take the free-running power output  $P_{\text{osc}} \approx 0.5 P_{\text{th}}$ . For a four-level system (e.g., Rhodamine-6G),  $N_{2\text{th}} \approx \Delta N_{\text{th}}$ . Using these approximations, we obtain

$$\Delta\omega_{\text{osc}} = \frac{\omega_0^3 \sigma_e \tau}{9 \ln(1/L_{\text{loss}}) c \lambda_p Q^2}. \quad (8)$$

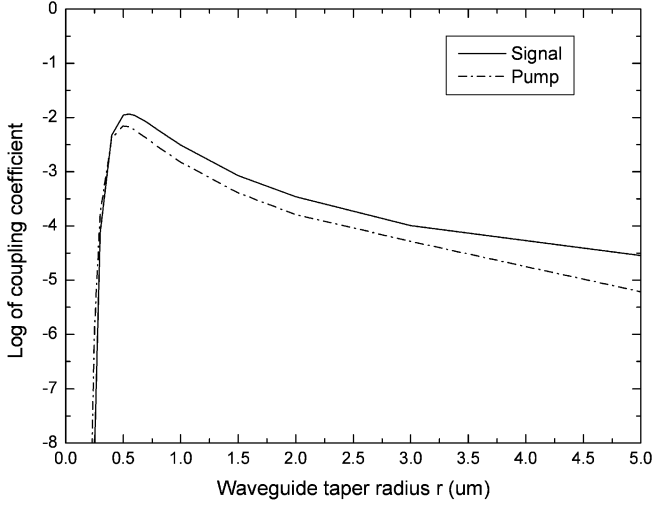


Fig. 2. Calculated coupling coefficient  $\kappa^2$  versus the radius  $r$  of the tapered waveguide for both pump and signal wavelengths.

There are mainly two types of losses in the microsphere resonator: 1) intrinsic loss including absorption, scattering, and radiation and 2) coupling loss between waveguide and microsphere. Here we take the coupling loss to be the dominating loss mechanism in the microcavity. In our design, the phase between the tapered waveguide and the WGM modes was optimized for the pump wave. Taking the radius of the microsphere  $R = 100 \mu\text{m}$ , we can obtain the relation of the coupling coefficient  $\kappa^2$  versus the radius of the waveguide taper region based on the coupled mode theory [6], and the results are shown in Fig. 2. Here the computation is carried only for the fundamental WGM laser mode.

From the preceding analysis and Fig. 2, we find the coupling coefficient at the signal (or lasing) wavelength to be approximately  $\kappa^2 = 0.01$ , which corresponds to a transmission coefficient  $t^2$  of 0.99. Consider the fact that the microsphere laser supports traveling waves in both directions; the total coupling loss is, therefore, given by  $2\kappa^2 = 0.02$ . Assuming that the coupling-induced cavity loss is much larger than the intrinsic cavity loss, we have  $L_{\text{oss}} = 1 - 2\kappa^2 = 0.98$ . Consequently, from (4) and (6), we can obtain the population inversion density  $\Delta N_{\text{th}} = 2.68 \times 10^{15} \text{ cm}^{-3}$ , and the threshold pumping power  $P_{\text{th}} = 0.86 \text{ mW}$ . By taking a moderate passive  $Q = 5 \times 10^5$  for the microsphere (using (3) with  $R = 100 \mu\text{m}$  and  $\kappa^2 = 0.01$ ), we get  $\Delta\omega_{\text{osc}} = 210.8 \text{ kHz}$  according to (8), and therefore an active  $Q_a = \omega/\Delta\omega_{\text{osc}} \rightarrow 10^{10}$ . This result shows that compared with a passive microsphere resonator, an active microsphere with gain can provide more than  $10^4$ -fold narrower linewidth in the transmission spectrum. It is with such greatly enhanced  $Q$  factors that we anticipate higher sensitivity for the active sensor.

### B. Frequency Shifts and Effective Index Changes

In the following, the relation between the spectrum line shift and the index change of the surrounding environment is given based on the perturbation approximation and mode volume evaluation. Firstly, let us consider the change of propagation

constant  $\Delta\beta$  due to the perturbation of the refractive indices. The change of propagation constant is related to the field profile of the propagating wave, and in the presence of index perturbation is described by [13]

$$\Delta\beta = \Delta n_e k = (\eta \cdot \Delta n_s + (1 - \eta) \cdot \Delta n_0) k \quad (9)$$

where  $n_e$  is the effective refractive index of the propagating mode, and  $\eta = \int_{\text{cavity}} |\psi|^2 da / \int_{\text{total}} |\psi|^2 da$  is the fraction of power inside the microcavity. For a microsphere cavity with radius  $R$ , there exists the standing wave condition that determines the resonance condition

$$\frac{\lambda}{n_e} l \cong 2\pi R \quad (10)$$

where  $l$  is the mode number, and we ignore the small frequency pulling effect associated with the atomic gain susceptibility [11] because the molecular linewidth of the dye is quite broad. Consider the frequency shift due to the change of effective refractive index. Within one free spectral range (FSR), we have

$$\frac{\Delta n_e}{n_e} = \frac{\Delta\lambda}{\lambda} = \frac{\Delta\omega}{\omega}. \quad (11)$$

In other words,  $\Delta n_e \sim n_e/Q_a$ . According to the analysis in the previous section for a passive microsphere with a moderate  $Q = 5 \times 10^5$ , the gain doped active microsphere can achieve a lasing linewidth  $\Delta\omega = 210.8 \text{ kHz}$  (i.e., the active  $Q_a \approx 10^{10}$ ), and the response of such an active microcavity to an effective index change of the order of  $10^{-10}$  can be detected. As compared with the conventional integrated optical waveguide sensor or surface plasmon resonance sensor [14], this represents a several orders of magnitude decrease in detection limit.

It is instructive to consider the possible nonlinear optical effect associated with such an active microcavity, because it could place a limit on the detectable refractive index change. We note that the third-order nonlinear susceptibility for a typical polymer  $\chi^{(3)} \sim 10^{-20} (\text{m}^2/\text{V}^2)$ . For the case we considered here, where the threshold pump power is  $0.86 \text{ mW}$  with a cross section of about  $3(\lambda_p)^2$ , the corresponding refractive index change due to material nonlinearity is about  $\Delta n_e \sim 10^{-9}$ . However, the nonlinear refractive index change can be affected by the pump light fluctuation rather than the average pump light intensity. In an actual experiment of sensing analytes, one can first measure the spectrum of microsphere in pure water as a reference, and then measure the spectrum with analytes in the water. By taking the difference of the resonance shifts, one can, in principle, eliminate the contribution of a possible nonlinear optical effect if the pump power is stabilized. In what follows, we will consider the detection limit to be limited to the order of  $10^{-9}$  due to the optical Kerr effect. In addition, the assumption we made earlier about neglecting the modification of dispersion relationship of the microcavity by the analytes can also be justified because the frequency shift due to analyte perturbation is within one free spectral range and on the order of only  $\Delta\omega \sim 10^5$ . One can easily choose an operating frequency that is outside the strong absorption range of the analytes.

In chemical and biological sensing applications, the small change in the effective refractive index could correspond to the presence of chemical or biological analytes of very low concentrations in the surrounding water environment (i.e., the measurand is homogeneously distributed) or bound to the microsphere surface (the measurand is equivalent to a thin film coating over the microsphere surface). For simplicity, we will consider a homogeneous index perturbation of the surrounding environment (the sensor then acts as a differential refractometer), where we will have  $\Delta n_e = (1 - \eta) \cdot \Delta n_0$ . Thus, the frequency shift of WGM resonances with the uniform change of surrounding refractive index at lasing condition can be expressed as

$$\frac{\Delta\omega}{\omega} = \frac{\Delta\lambda}{\lambda} = (1 - \eta) \frac{\Delta n_0}{n_e}. \quad (12)$$

Calculation shows that  $\eta = 0.99$  for a microsphere with  $R = 100 \mu\text{m}$  and  $\lambda = 0.58 \mu\text{m}$  at the fundamental modes. Equation (12) tells us that an active microsphere sensor can detect an index change of the order  $10^{-7}$  in the surrounding water solution for  $\Delta n_e \sim 10^{-9}$ . In practice, care has to be taken to avoid any unintended fluctuations that could also result in refractive index change, e.g., by careful control of the temperature and enclosing the sensor in microfluidic chambers. For biosensor applications, the target biomolecules will bind to the microsphere surface via specific receptors. The device should give a more sensitive response to the binding of molecules than those present in the surrounding environment. The design considerations are beyond the scope of this paper, and readers are referred to more detailed treatment [14], [15].

Finally, we point out that we used a very relaxed criterion to distinguish the spectrum peak shift (i.e., to detect the shift by the FWHM of the peak). In reality, a small fraction of the FWHM can be easily detected. On the other hand, detection can also be made by fixing the wavelength and measuring the output intensity variation due to the shift of the resonance position [4]. In the latter case, the sensitivity will be determined by the minimum power detection limits. If we use shot-noise limited power as the criterion for the minimum power as discussed in [16], a much lower detection limit in the index change can be established by using an active microcavity sensor.

### III. DESIGNS OF A MICROSPHERE COUPLED WITH A CYLINDRICAL WAVEGUIDE

The sizes of the microsphere and waveguide taper (Fig. 3) are critical parameters for the sensor to achieve the desired sensitivity. We will calculate in detail the intrinsic  $Q(Q_{\text{in}})$  and the external  $Q(Q_{\text{ex}})$  of polystyrene microspheres. The intrinsic  $Q$  is related to the loss from absorption, scattering and radiation, whereas the radiation loss is induced by the curvature of the spheres. In our discussion, the scattering loss is ignored because the surface of the microsphere can be extremely smooth; the material absorption loss is taken into account for the upper limit of passive  $Q$  factor. By calculating  $Q_{\text{in}}$ , we can find the minimal size of a microsphere needed to provide a suitable  $Q$  for the sensors. The external  $Q$  is determined by the coupling coefficient between the microsphere and the cylindrical waveguide. By

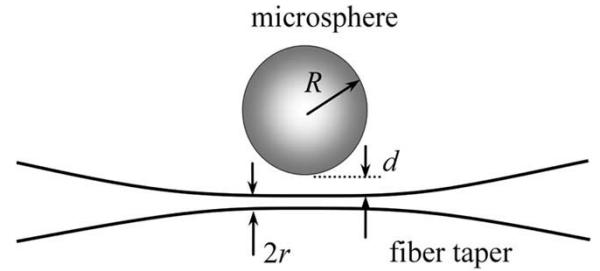


Fig. 3. Configuration of a microsphere and waveguide taper coupling system, where  $R$  is the radius of the microsphere,  $r$  the radius of the tapered fiber and  $d$  the gap distance between the microsphere and the fiber taper. Both pump and signal light are introduced from the same input port of the fiber.

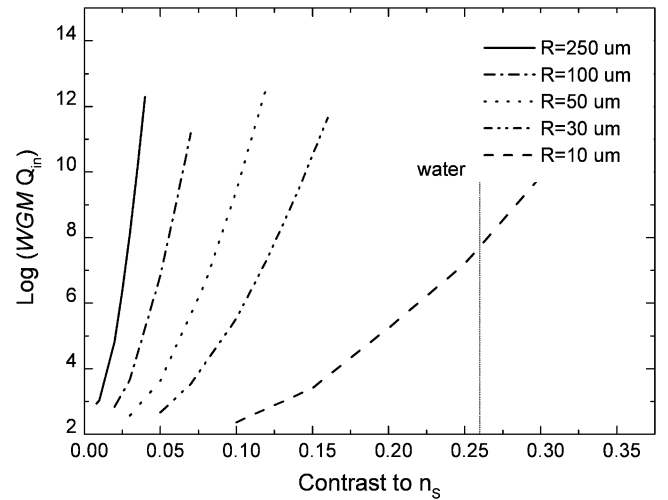


Fig. 4. The limiting  $Q_{\text{in}}$  values due to WGM loss as a function of index contrast between the microsphere and the surrounding water.

analyzing the relationship between  $Q_{\text{ex}}$  and the radius of the tapered waveguide at the coupling region, we can determine the optimal size of waveguide taper.

Using the volume-current method presented in [6], we calculated the limiting  $Q_{\text{in}}$  due to the radiation loss of the fundamental WGM mode as a function of index contrast between the polymer microsphere ( $n_s$ ) and that of the surrounding environment ( $n_0$ ). The results are plotted in Fig. 4. It is clear that one should select a sphere radius  $R \geq 10 \mu\text{m}$  in order to achieve  $Q \geq 10^6$  for desired sensitivity. In Fig. 4, the dashed line indicates the index contrast of 0.26 between water and polystyrene. Additionally, it should be noted that the light absorbance loss in microspheres also provides another limit  $Q_l$  on the quality factor. Typically, the absorption coefficient of light at  $\lambda = 0.58 \mu\text{m}$  in polymer fiber is less than 1 dB/m; this implies that  $Q_l > 10^7$ .

The optimal coupling of the microsphere and the fiber taper can be obtained by evaluating the relation of the external  $Q(Q_{\text{ex}})$  and the radius of the tapered fiber. Using the coupled mode method [6], we calculated  $Q_{\text{ex}}$  as a function of the minimum waist of the waveguide taper for the fundamental WGM of microspheres with radius of  $100 \mu\text{m}$  and  $50 \mu\text{m}$ , respectively. It is assumed that the microsphere is in direct contact with the taper (i.e.,  $d = 0$  in Fig. 3). For comparison, we also simulated the ideal case in which perfect phase matching is assumed,

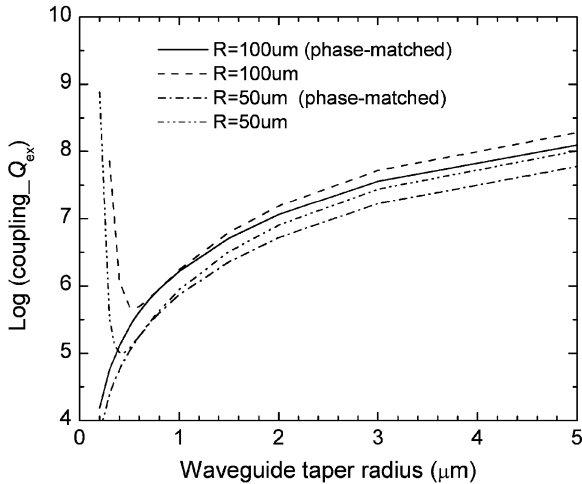


Fig. 5. External  $Q_{ex}$  as a function of the taper waist radius. For comparison, the case assuming phase matching is also shown.

i.e., the propagation constants of the fundamental WGM and the waveguide taper are the same for any given taper radius. From Fig. 5, one can find the optimal coupling parameters for the tapers to achieve the maximum coupling coefficients for signal wavelength at  $\lambda = 0.58 \mu\text{m}$ . For  $R = 100 \mu\text{m}$ , the taper radius  $r$  should be  $\sim 0.6 \mu\text{m}$ ; and for  $R = 50 \mu\text{m}$ ,  $r$  should be  $\sim 0.4 \mu\text{m}$ . Note that to achieve low threshold pumping, we need to optimize the coupling condition to get maximum coupling coefficients for the pumping wavelength, but not necessarily for the signal wavelength. In our case, the corresponding optimal taper sizes for both pumping and signal lights are close to each other (see Fig. 2).

#### IV. CONCLUSION

We have shown that by using microsphere resonators with gain, one can potentially obtain greatly improved sensitivity to the effective refractive index changes by virtue of the very narrow resonance linewidth at the lasing condition. In order to detect a resonance shift due to index perturbation, one needs a high-resolution spectrometer to measure the linewidth. Alternatively, one can measure the output intensity change at a fixed wavelength within the resonance peak. Although the analysis is presented for the case of gain-doped microsphere coupled with a tapered fiber, a similar analysis can be applied to a planar microring or microdisk coupled with an integrated optical waveguide. For example, by doping the polymer microring resonators demonstrated in [4] with gain media such as dyes, one could take the advantage of simple and low-cost fabrication methods such as imprinting [17] or molding [18] to implement integrated sensor arrays to detect analytes with very low concentrations.

#### REFERENCES

[1] B. E. Little, S. T. Chu, and H. A. Haus, "Second-order filtering and sensing with partially coupled traveling waves in a single resonator," *Opt. Lett.*, vol. 23, pp. 1570–1572, 1998.  
 [2] F. Vollmer, D. Braun, A. Libchaber, M. Khoshshima, I. Teraoka, and S. Arnold, "Protein detection by optical shift of a resonant microcavity," *Appl. Phys. Lett.*, vol. 80, pp. 4057–4059, 2002.

[3] R. W. Boyd and J. E. Heebner, "Sensitive disk resonator photonic biosensor," *Appl. Opt.*, vol. 40, pp. 5742–5747, 2001.  
 [4] C. Y. Chao and L. J. Guo, "Biochemical sensors based on polymer microrings with sharp asymmetrical resonance," *Appl. Phys. Lett.*, vol. 83, pp. 1527–1529, 2003.  
 [5] A. Yariv, "Universal relations for coupling of optical power between microresonators and dielectric waveguides," *Electron. Lett.*, vol. 36, pp. 321–322, 2000.  
 [6] B. E. Little, J. -P. Laine, and H. A. Haus, "Analytic theory of coupling from tapered fibers and half-blocks into microsphere resonators," *J. Lightw. Technol.*, vol. 17, no. 4, pp. 704–715, Apr. 1999.  
 [7] D. K. Armani, T. J. Kippenberg, S. M. Spillane, and K. J. Vahala, "Ultra-high-Q toroid microcavity on a chip," *Nature*, vol. 421, pp. 925–928, 2003.  
 [8] D. A. Cohen, E. J. Skogen, H. Marchand, and L. A. Coldren, "Monolithic chemical sensor using heterodyned sampled grating DBR lasers," *Electron. Lett.*, vol. 37, pp. 1358–1360, 2001.  
 [9] F. J. Duarte and L. W. Hillman, *Dye Laser Principles*. New York: Academic, 1990.  
 [10] M. Cai, O. Painter, K. J. Vahala, and P. C. Sercel, "Fiber-coupled microsphere laser," *Opt. Lett.*, vol. 25, pp. 1430–1432, 2000.  
 [11] A. E. Siegman, *Lasers*. Mill Valley, CA: University Science, 1986.  
 [12] M. Cai, "Optical Fiber Coupled Glass Microsphere Resonators," Ph.D. dissertation, Dept. Appl. Phys., California Inst. Technol., Pasadena, CA, 2001.  
 [13] A. W. Snyder and J. O. Love, *Optical Waveguide Theory*. New York: Chapman & Hall, 1983.  
 [14] P. A. Lowe, T. J. H. Alwyn Clark, R. J. Davies, P. R. Edwards, T. Kinning, and D. Yeung, "New approaches for the analysis of molecular recognition using the IASys evanescent wave biosensor," *J. Mol. Recognit.*, vol. 11, pp. 194–199, 1998.  
 [15] O. Parriaux and G. J. Veldhuis, "Normalized analysis for the sensitivity optimization of integrated optical evanescent-wave sensors," *J. Lightw. Technol.*, vol. 16, no. 4, pp. 573–582, Apr. 1998.  
 [16] E. Krioukov, J. Greve, and C. Otto, "Performance of integrated optical microcavities for refractive index and fluorescence sensing," *Sens. Actuators B, Chem.*, vol. 90, pp. 58–67, 2003.  
 [17] C. Y. Chao and L. J. Guo, "Polymer micro-ring resonators fabricated by nanoimprint technique," *J. Vac. Sci. Technol. B, Microelectron.*, vol. 20, pp. 2862–2866, 2002.  
 [18] A. L. Martin, D. K. Armani, L. Yang, and K. J. Vahala, "Replica-molded high-Q polymer microresonators," *Opt. Lett.*, vol. 29, pp. 533–535, 2004.

**Jun Yang** received the B.S. degree in optical engineering from Beijing Institute of Technology, Beijing, China, in 1994. He is currently pursuing the Ph.D. degree in electrical engineering at the University of Michigan, Ann Arbor.

His research interests include integrated optoelectronics, organic photonics, and nanofabrication technology.



**L. Jay Guo** (S'96–M'97) received the B.S. degree in biophysics from Nankai University, China, in 1990, and the Ph.D. degree in electrical engineering from the University of Minnesota, Minneapolis, in 1997.

He was a Research Associate at Princeton University from 1998 to 1999. He joined the University of Michigan, Ann Arbor, in 1999, and is currently an Associate Professor in the Department of Electrical Engineering and Computer Science. His research areas include organic electronics, nanoimprinting, nanophotonics, nanofabrication technologies with applications in polymer photonic devices, and biotechnologies.